

1 **Wind speed affects the rate and kinetics of stomatal conductance**

2
3 Or Shapira^{1,2}, Uri Hochberg³, Scott McAdam⁴, Tamar Azoulay-Shemer², Craig R. Brodersen⁵,
4 Noel Michelle Holbrook⁶, Yotam Zait⁷

- 5
6
7 1. Golan Research Institute, P.O. Box 97, Katzrin 12900, Israel
8
9 2. Fruit Tree Sciences, Agricultural Research Organization (ARO), The Volcani Center,
10 Newe Ya'ar Research Center, Ramat Yishay, 30095, Israel.
11
12 3. ARO Volcani Center, Institute of Soil, Water and Environmental Sciences, Rishon
13 Lezion, 7505101 Israel.
14
15 4. Purdue Center for Plant Biology, Department of Botany and Plant Pathology, Purdue
16 University, West Lafayette, IN 47907, USA.
17
18 5. School of the Environment, Yale University, New Haven, CT 06511, USA.
19
20
21 6. Department of Organismic and Evolutionary Biology, Harvard University, 26 Oxford St,
22 Cambridge, MA, 02138 USA.
23
24
25 7. The Robert H. Smith Institute of Plant Sciences and Genetics in Agriculture, Faculty of
26 Agriculture, Food and Environment, The Hebrew University of Jerusalem, Rehovot
27 76100, Israel.

28
29
30 Corresponding author: Yotam Zait, Email: yotam.zait@mail.huji.ac.il

31
32
33
34
35
36

37

38 **Abstract**

39 Understanding the relationship between wind speed and gas exchange in plants is a longstanding
40 challenge. Our aim was to investigate the impact of wind speed on maximum rates of gas
41 exchange and the kinetics of stomatal responses. We conducted experiments using an infrared
42 gas analyzer equipped with a controlled leaf fan, enabling precise control of the boundary layer
43 conductance. We first showed that the chamber was adequately mixed even at extremely low fan
44 speeds (down to 200 rpm, equivalent to a wind speed of 0.0005 m s^{-1}) and evaluated the link
45 between fan speed, wind speed, and boundary layer conductance. We observed that higher wind
46 speeds led to increased gas exchange of both water vapor and CO_2 in *Arabidopsis*, presumably
47 due to its effect on transpiration and the consequential reduction in epidermal pressure that led to
48 stomatal opening. We documented that stomatal opening in response to light was three times
49 faster at a fan speed of 10000 rpm (wind speed of 2 m s^{-1}) compared with 500 rpm (0.25 m s^{-1}) in
50 *Vicia faba*, while the latter exhibited an opening rate that was similar to those of epidermal peels.
51 The increase of stomatal conductance under high wind was observed in four species under field
52 conditions. Our findings demonstrate the importance of the size of the boundary layer on
53 determining maximum rates of gas exchange and the kinetics of gas exchange responses to
54 environmental changes.

55

56 **Keywords:** Transpiration, Stomata, gas exchange, wind, boundary layer, leaf fan

57

58

59

60

61

62

63

64

65

66

67

68

69

70

71 **Introduction**

72 Stomatal pores play a critical role in regulating gas exchange between a plant and its
73 environment, affecting both photosynthesis and transpiration. The aperture of stomatal pores is
74 influenced by various environmental factors, including light, humidity, temperature and
75 atmospheric CO₂ (Assmann & Jegla, 2016; Kim et al., 2010; Kollist et al., 2014; Shimazaki et
76 al., 2007). It has been previously suggested that wind influences transpiration through a direct
77 effect on the boundary layer (Aphalo & Jarvis, 1993; Foster & Smith, 1986), but the wind effect
78 that is mediated through stomatal regulation is far less explored and is absent from transpiration
79 models.

80 Wind is hypothesized to affect gas exchange in two ways. First, wind speed affects the boundary
81 layer, a thin layer of air adjacent to the leaf surface, where the gas flow is dominated by shearing
82 forces, resulting from the interaction between the leaf and the surrounding air (Cowan, 1978).
83 The thickness of this boundary layer is mainly influenced by local wind speed and leaf size, with
84 leaf shape having a secondary effect (Nobel, 2020). The thickness of the boundary layer impacts
85 transpiration, as it determines the resistance to water vapor diffusion from the stomatal pores to
86 the surrounding atmosphere (Nobel, 2020). Low wind speeds lead to a thick boundary layer, and
87 its resistance could become dominant with respect to transpiration in winds lower than 0.25 m s⁻¹
88 (Foster & Smith, 1986). Absent or very low speed winds are relatively common in dense
89 canopies of forests (Renaud et al., 2011) or crops (Shaw, 1977). Plants can indirectly control
90 boundary layer conductance through modifications to morphology, size, and leaf orientation,
91 which in turn affects flow patterns. While the variability within canopies and among species
92 could be substantial, the interaction between wind speed, the boundary layer, and its direct effect
93 on transpiration is well accepted (Nobel, 2020).

94 The second effect, which is the focus of this current research, is far less explored. Swift changes
95 to boundary layer conductance (g_b) caused by altered wind speed has the potential to result in
96 rapid changes to leaf evaporation rate and thus leaf water status. Stomatal responses to changes
97 in transpiration rate can be both actively and passively regulated (Franks, 2013). Active stomatal
98 responses are a function of ion pumping or efflux, resulting in changes in guard cell osmotic
99 potential (Kearns & Assmann, 1993). Passive movement, on the other hand, is a faster response
100 that occurs as a consequence of changes in leaf water status (Buckley, 2005; McAdam &
101 Brodribb, 2014; Meidner & Heath, 1963; Zait et al., 2017). In angiosperms the passive response
102 is governed by the turgor of the epidermal cells which have a mechanical advantage over the
103 guard cells (DeMichele & Sharpe, 1973; Mott & Franks, 2001; Buckley *et al.*, 2011). If a rapid
104 increase in transpiration rate causes turgor pressure to decrease in both the epidermal cells and
105 guard cells (Franks et al., 1998), the stomata will open (Franks & Farquhar, 2007), resulting in a
106 passive stomatal opening (Frensch & Schulze, 1988; Raschke, 1970). This passive mechanism
107 also closes the pore when transpiration rate decreases rapidly and epidermal backpressure
108 increases (Zait et al., 2017). We do not know the effect g_b on potential changes to epidermal cell
109 turgor and thus stomatal sensitivity to environmental changes. There is very little work that has

110 investigated whether epidermal cell turgor alters stomatal sensitivity to environmental changes
111 (Franks and Farquhar 2007).

112 In this study, we investigate the relationship between wind speed and transpiration to disentangle
113 the effects of the boundary layer on gas exchange. We relate wind speed inside the gas exchange
114 chamber to g_b and examined stomatal responses to light under different wind speeds. We
115 hypothesize that in angiosperms, increasing transpiration by increasing wind speed and thus
116 decreasing g_b will result in both a passive increase in stomatal conductance and an increase in the
117 rate of stomatal opening in response to light.

118 **Materials and Methods**

119 We performed three experiments using the LI-6800 (LI-COR Biosciences, Lincoln, NE, USA).
120 The first experiment was designed to test whether under a very low fan speed there is sufficient
121 mixing to accurately measure gas exchange. In the second experiment, we linked the fan speed to
122 wind speed using an omnidirectional air velocity transducer and determined g_b by determining
123 evaporation from wet filter paper inside the chamber. The third set of experiments was
124 conducted on *Vicia faba* and *Arabidopsis*, under controlled conditions, and four angiosperm
125 species growing outside, to evaluate the effect of different wind speeds on plant gas exchange.

126 ***Plant material and growth conditions***

127 The *Vicia faba* and *Arabidopsis* plants used in this study were grown under controlled
128 environmental conditions. *Vicia faba* were planted in 5 L pots, growth chamber maintained at a
129 temperature range of 22-25°C during the day and 18-20°C at night, under a daytime light
130 intensity of 300 $\mu\text{mol m}^{-2} \text{s}^{-1}$. The relative humidity within the growth chamber was maintained
131 at 60-70% to ensure adequate moisture availability for the plants and prevent excessive
132 transpiration. *Arabidopsis* (Columbia, Col-0) seeds were planted in 250 ml pots filled with a soil
133 mixture (Green 20, Even Ari, Israel) + 2 g/L Osmocote. Plants were grown in a growth chamber
134 under a light intensity of 250 $\mu\text{mol s}^{-1} \text{m}^{-2}$ and a 12 h photoperiod. The temperature was
135 maintained at 21°C during the day and 19°C at night, with a relative humidity (RH) ranging
136 between 60% during the day and 85% at night.

137 To test the response to wind speed in plants that are growing outdoors, and have thus
138 experienced a far more diverse wind regimes, we measured four plant species growing at
139 Zemach Nisyonot research farm on experimental plots: mango (*Mangifera indica*), papaya
140 (*Carica papaya*), *Withania somnifera*, and fig (*Ficus carica*). All the measured plants were fully
141 watered and in a healthy state.

142 ***Gas exchange measurements***

143 Gas exchange measurements were conducted using a LI-6800F portable photosynthesis system
144 (LI-COR Biosciences, Lincoln, NE, USA). This system is equipped with a leaf chamber of 2 cm^2
145 and an infrared gas analyzer (IRGA) to measure CO_2 assimilation rate, transpiration rate (E), and
146 other climatic parameters in real-time. On the day of the experiment, a healthy, fully expanded
147 leaf was selected for measurements. The leaf was carefully inserted into the leaf chamber, and
148 the system was set to control all environmental parameters including light intensity, temperature,

149 relative humidity, and CO₂ concentration (see details below). The leaf fan speed was adjusted in
150 the chamber to manipulate boundary layer conductance during the experiment.

151 *Evaluation of mixing in the LI-6800F chamber*

152 In this experiment, we employed a methodology that closely followed the approach of McNab
153 (2006) for measurements of animal respiration. A mature mango leaf, attached to the plant, was
154 placed into a LI-COR 6800F cuvette and subjected to an hour of dark adaptation until a stable
155 dark respiration rate was achieved. We then set the flow rate to 950 $\mu\text{mol s}^{-1}$ for five minutes,
156 recording the respiration rate every five seconds. Following this, we reduced the flow rate to
157 around 850 $\mu\text{mol s}^{-1}$ for an additional five minutes. This procedure was repeated at ten lower
158 flow rates, down to 20 $\mu\text{mol s}^{-1}$. The procedure was repeated at four fan speeds (200, 800, 2000,
159 and 10,000 rpm), with the aim of observing a reciprocal linear relationship between respiration
160 rate and flow rate, to verify adequate air mixing within the chamber (McNab, 2006). Any
161 deviation from a linear relationship between respiration rate and either fan speed or flow rate
162 would suggest inadequate gas mixing. We identified the critical flow rate for each fan speed,
163 defined as the minimum flow rate necessary for comprehensive gas mixing in the chamber.

164

165 *Wind speed measurements*

166 Wind speed was measured using an omnidirectional air velocity transducer (model 8475, TSI,
167 Singapore) placed inside the leaf chamber and connected directly to an auxiliary channel through
168 the 25-pin connector on the of the LI-6800F. The voltage from the sensor was transformed to
169 wind speed in m s^{-1} according to the user manual. The data was logged into the gas exchange
170 results file. Fan speed was changed from 200 rpm up to 10000 rpm at 200 rpm increments for 4
171 min at each speed. The data was logged every 15 s. The mean of the last 15 observations from
172 each step were averaged. This test was repeated nine times at different angles of the sensor inside
173 the measuring chamber, and averaged. The measuring probe was directed to be in the center of
174 the 2 cm^2 round chamber parallel to the leaf plane. Flow rate was adjusted to 500 $\mu\text{mol s}^{-1}$. The
175 area around the sensor rod and the leaf chamber interface was sealed with dental epoxy to
176 prevent leaks.

177 *Measurement and calculation of boundary layer conductance*

178 Rates of water loss from filter paper (Whatman no.3) saturated with distilled water have been
179 used to calculate the boundary layer conductance for water vapor (g_b) (Parkinson, 1985). This
180 experimental approach provides a means to estimate g_b of unadorned leaves under the conditions
181 inside the chamber without the interference of stomata. Chamber temperature (T_{exchange}) was set
182 to 22 °C, T filter paper was 19.7±0.9 °C, RH= 50%, VPD~0.74±0.09 kPa, and the flow rate was
183 630 $\mu\text{mol s}^{-1}$. The leaf thermocouple was touching the filter paper. Fan speed was changed from
184 0 to 300 rpm and then to 10000 rpm in increments of 200 rpm, with 4 min at each fan speed.
185 Evaporation rate was logged every 4 s. The H₂O IRGA was matched every 5 min and points
186 around the match event were excluded from the results. The boundary layer ;proportion of total

187 conductance (g_t) was calculated by the LI-6800F according to the equation: $g_t = \frac{E \left(1 - \left(\frac{w_i - w_a}{2}\right)\right)}{w_i - w_a}$
188 where E is the transpiration and w_i is the water saturation in the wet filter paper and the w_a is
189 the water concentration in the air.

190 ***Evaluation of boundary layer conductance and wind speed effects on gas exchange*** 191 ***measurements***

192 To examine the effect of fan speed on transpiration (E) g_s , steady-state measurements of g_s and E
193 were conducted on 6-week-old Arabidopsis plants. The leaves were stabilized in the chamber
194 under 60% RH, $T_{\text{exchange}} = 22^\circ\text{C}$, PAR $350 \mu\text{mol m}^{-2} \text{s}^{-1}$, flow rate $530 \mu\text{mol s}^{-1}$ and fan speed of
195 1000 rpm (wind speed of 0.03 m s^{-1}). Data was recorded every 30 s. The fan speed was then
196 increased to 10000 rpm (wind speed of 2 m s^{-1}). These measurements were performed at a low
197 CO_2 concentration of 100 ppm to ensure stomata were open and reduce any effect of increasing
198 internal CO_2 concentration on stomatal movements.

199 Gas exchange measurements were also carried out to assess the impact of gradual changes in
200 wind speed. The wind speed was gradually (linearly) increased over a 5-min interval by
201 incrementally adjusting the fan speed from 200 rpm (corresponding to 0.005 m s^{-1}) to 7000 rpm
202 (equivalent to 1.5 m s^{-1}). Values were logged every 30 s. Other conditions in the chamber were
203 as described in the previous paragraph.

204 To assess the influence of wind speed on the kinetics of stomatal opening in the transition from
205 dark to light, we conducted experiments with three different fan speeds (500, 1000, and 10000
206 rpm) while maintaining the plants in dark conditions and subsequently exposing them to light at
207 an intensity of $800 \mu\text{mol m}^{-2} \text{s}^{-1}$. Stomatal conductance was measured throughout this transition,
208 and we compared the rates of change in gas exchange (stomatal conductance) with the stomatal
209 aperture observed in epidermal peels submerged in a buffer solution derived from the same
210 leaves that were measured (see below the stomatal aperture assay). To facilitate comparison, we
211 converted the data to a percentage of stomatal opening $[(g_s \text{ max} - g_s) / g_s \text{ max}]$.

212 In the common garden experiment, measurements were conducted under the following chamber
213 environmental conditions: a flow rate of $700 \mu\text{mol s}^{-1}$, PAR $2000 \mu\text{mol m}^{-2} \text{s}^{-1}$, a temperature
214 of 36°C , and a relative humidity of 45%. We tested every species when wind speed was
215 increased in one step change from 0.05 m s^{-1} to 1.5 m s^{-1} and to 2.5 m s^{-1}

216 ***Stomatal aperture assay***

217 Fully expanded *Vicia faba* leaves were harvested from 4-week-old plants grown under controlled
218 environmental conditions. These plants were the same ones used for gas exchange measurements
219 with the LI-6800F system. Epidermal peels were prepared using a gentle peeling technique to
220 ensure the integrity of the stomatal complexes (Zhu et al., 2016). Initially, the epidermal peels
221 were incubated in darkness for 1.5-2 hours in a buffer solution containing 5 mM KCl, 1 mM
222 CaCl_2 , and 10 mM MES-KOH (pH 6.15). After this incubation period, the peels were transferred
223 to the light ($400 \mu\text{mol m}^{-2} \text{s}^{-1}$) with 50 mM KCl and 0.1 mM CaCl_2 . Stomatal apertures were then
224 measured using a light microscope ECHO (Rebel, Bico Company, San Diego, USA)

225

226 **Results**

227 ***Evaluation of mixing in the LI-6800F chamber***

228 We first sought to determine the minimum fan speed in the cuvette of the gas analyzer that could
229 provide sufficient mixing so that gas exchange could be accurately measured. We assessed the
230 mixing inside the LI- 6800F chamber by measuring leaf respiration in the dark across flow rates
231 and fan speeds (**Fig. 1**). Because dark respiration is independent of chamber flow rate and fan
232 speeds under adequate air mixing conditions within the chamber, a reciprocal linear relationship
233 should exist between flow rate and ΔCO_2 . This quantitative reciprocity defines the range of flow
234 rates (at different fan speeds) for which gases in the chamber are sufficiently mixed, ensuring
235 that the calculated rates of gas exchange are reliable estimates. To investigate the impact of fan
236 speeds on air mixing within a leaf chamber, the flow rate was adjusted from ~ 950 to $\sim 50 \mu\text{mol s}^{-1}$
237 $^{-1}$, while maintaining constant fan speeds at 200, 800, 2000, and 10000 rpm (**Fig. 1**). We
238 monitored the differences in CO_2 mole fraction (μmol) under these conditions. The results
239 revealed a significant effect of the flow rate on the curvature patterns and standard deviation
240 associated with CO_2 mole fraction differences. Within the observed data, a distinct linear region
241 represented the range where reliable measurements of gas exchange could be obtained,
242 indicating adequate air mixing. However, critical flow rates were identified, beyond which air
243 mixing was compromised, leading to nonlinearity in the relationship. The slope of the
244 relationship between flow rate and CO_2 differential remained consistent across tested fan speeds,
245 (**Figure S1**).

246

247 ***Measurement of wind speed and boundary layer conductance inside the LI-6800F chamber***

248 We next examined wind dynamics inside the LI-6800F chamber (**Fig. 2**). Gas exchange analysis
249 revealed that fan speed increments from 0 up to 1000 rpm had a minor effect on wind speed
250 (change from 0.005 to 0.029 m s^{-1}), while a change in fan speed from 1000 to 10000 rpm
251 increased wind speed linearly (at a slope of 0.0002 m s^{-1} per rpm) reaching 2 m s^{-1} at 10000 rpm.
252 To further clarify the effect of g_b on transpiration, while eliminating the confounding effect of g_s ,
253 we measured the transpiration rate from a wet filter paper under dark conditions. The response of
254 boundary layer conductance ($g_{b \text{ filter paper}}$) was divided into 2 linear sections. First, at fan speeds
255 from 300 rpm to 3100 rpm $g_{b \text{ filter paper}}$ increased from 0.16 to $1.42 \text{ mol m}^{-2} \text{ s}^{-1}$ (slope of 0.0005
256 $\text{mol m}^{-2} \text{ s}^{-1}$ per rpm), and second from 3100 to 10000 rpm $g_{b \text{ filter paper}}$ increased up to 2.4 mol m^{-2}
257 s^{-1} (slope of $0.0001 \text{ mol m}^{-2} \text{ s}^{-1}$ per rpm). It's important to note that some discrepancies exist
258 between our estimation of the boundary layer conductance and the conductance calculated by the
259 LI-6800F at fan speeds lower than 1900 rpm and higher than 4000 rpm. We therefore replaced
260 the values of the boundary layer conductance in the LI-6800F data sheet used to calculate g_s with
261 the data obtained by the filter paper method in our measurements. In addition to estimating g_b
262 using the filter paper we calculated the width of the boundary layer in the 6800F 2 cm^2 chamber
263 according to the relationship:

264 g_b (mm) = $4 * \sqrt{l_{(m)}} / v_{(ms^{-1})}$ (Equation 7.10 Nobel 2009) where $l_{(m)}$ is the diameter of the
265 chamber, $v_{(m s^{-1})}$ is the ambient wind speed at each fan speed as measured by us, and g_b (mm) is
266 the thickness of the boundary layer in mm. Next, we used the relationship $g_b = D^w / g_b$ (mm)
267 (Aphalo & Jarvis, 1993), where D^w is the diffusion coefficient of water in air to calculate the
268 approximate g_b in $\text{mol m}^2 \text{s}^{-1}$ for all wind speeds measured inside the chamber from fan speed of
269 200 rpm to 10000 rpm. The calculated data agreed well with our estimation only at the lower
270 range of fan speeds from 800 to 2700 rpm and with the original data calculated by the LI-6800
271 only in the higher part of the range above 2700 rpm (black line Fig. 1). At the very low range
272 (<800 rpm) the calculation diverged from both our measurements and the LI-6800 model.

273

274 **Manipulating wind speeds to modulate transpiration rates and vapor pressure deficit**

275 Changing the wind speed from 0.03 to 2 m s^{-1} resulted in g_s increasing from 0.33 to 0.51 mol m^{-2}
276 s^{-1} within one minute in *Arabidopsis* (Fig 3a). Our results indicate that by manipulating fan
277 speeds from 1000 to 10000 rpm we could induce changes in E (from 2.2 to $3.1 \text{ mmol m}^{-2} \text{ s}^{-1}$)
278 with an inverse effect on VPD (0.9 to 0.68 kPa) due to the cooling effect of the increased
279 transpiration. It important to note that the reverse effect (reduction in g_s in response to lower fan
280 speed) was also measured (Fig S2). These results demonstrate that higher g_s is linked to elevated
281 E resulting from enhanced g_b .

282 A gradual increase in wind speed over 5 min, ranging from 0.005 (fan speed of 200 rpm) to 1.5
283 m s^{-1} (fan speed of 7000 rpm) (Fig. 4a) corresponded to a progressive rise in g_s from 0.2 to 0.33
284 $\text{mol m}^{-2} \text{ s}^{-1}$. The gradual increment in wind speed resulted in an increase in E from 1.4 to 2.7
285 $\text{mmol m}^{-2} \text{ s}^{-1}$, accompanied by a decrease in VPD₁ from 1.2 to 0.95 kPa (Fig. 4b). The fact that
286 the increase in E actually changed g_s is demonstrated by the change in photosynthesis rate, which
287 increased from 8.2 to $11.2 \text{ } \mu\text{mol m}^{-2} \text{ s}^{-1}$ over the 5-min interval of wind speed increment (Fig.
288 4c). It is worth noting that the transpiration efficiency decreases by 31%, suggesting a more
289 pronounced impact on water vapor relative to assimilation in response to an increase in wind
290 speed.

291 ***Stomatal conductance response to light under different fan speeds***

292 We examined stomatal opening kinetics in the transition from dark to light in *Vicia faba*. We
293 compared three different fan speeds with stomatal opening observed in epidermal peels (Fig. 5).
294 We found a significant relationship between fan speed and the rate of stomatal opening. As fan
295 speed increased, the rate of stomatal opening also increased, suggesting that higher g_b is
296 associated with faster stomatal opening kinetics. Stomatal opening observed in epidermal peels
297 was similar to the opening seen during gas exchange measurements with fan speeds of 500 rpm,
298 but 14 and 63% slower compared to stomatal opening during gas exchange measurements with
299 fan speeds of 1000 and 5000 rpm, respectively.

300 ***Stomatal conductance response to increasing wind speed in various plant species***

301 We investigated the response of g_s to increasing wind speed in several plant species growing
302 under field conditions, including mango (*Mangifera indica*), papaya (*Carica papaya*), *Withania*

303 *somnifera* and fig (*Ficus carica*) (**Fig. 6**). We found a consistent enhancement in g_s for all
304 species as wind speed increased from 0.05 to 2.5 m s⁻¹. The inset in figure 6 shows the slopes of
305 the regression fits with their 95% CI. These findings highlight the impact of wind speed on
306 stomatal behavior across the different plant species studied.

307 **Discussion**

308 *Technical consideration for gas exchange measurements at low fan speeds*

309 Our results indicate that the LI-6800F gas exchange system's air mixing capability is not
310 compromised even under fan speed as low as 200 rpm and is mainly dependent on the air flow
311 rate rather than fan speed (**Fig. 1**). This flow-driven mixing should not come as a surprise if we
312 consider that an airflow rate above 500 $\mu\text{mol s}^{-1}$ in a chamber volume of 87 cm³, represents 12
313 complete air replacements every minute (1.1 L min⁻¹). It thus seems that the recommendation to
314 set the leaf fan to 10000 rpm (Using the LI-6800 v2.1 <https://www.licor.com/env/support/LI-6800/manuals.html>)
315 is not critical for accurate measurements of gas exchange. The ability to
316 measure gas exchange at low fan speed, combined with the versatile possibilities of fan speed
317 control provided by new gas exchange systems, opens a range of possibilities for studies of leaf
318 response to wind.

319 We found that the filter paper estimation of g_b did not always agree with g_b according to Nobel,
320 (2020) and was lower especially at fan speed above 2700 rpm (**Fig. 2**). One reason that our g_b
321 data was lower could be related to the pattern of the air flow across the leaf surface in the
322 chamber. The model proposed by Nobel centers the boundary thickness calculation on the
323 laminar flow of air where air movement is predominantly parallel to the leaf surface. In the gas
324 exchange chamber air movement cannot be absolutely parallel to the leaf surface due to the
325 geometry of the chamber air inlets. The leaf surfaces are sunk below the leaf gasket most likely
326 preventing the conditions required for the Nobel equation calculation. Another deviation could
327 result from the discrepancy between the mean length of the leaf in the direction of the wind (in
328 the model $l_{(m)}$) and the $l_{(m)}$ which we used as the diameter of the 2 cm² round chamber. Sub-
329 saturation of the filter paper leading to lower transpiration and interpreted as lower total
330 conductance (g_t) could also be a reason for the discrepancy between our results and Nobel,
331 (2020).

332 More importantly, our estimation of g_b diverged from the data supplied by the manufacturer (**Fig.**
333 **2**). We are not sure regarding the source of this error, but we would like to clarify that it probably
334 makes little significance with respect to past measurements. The vast majority of published
335 measurements were made at max fan speed (e.g., Barzilai et al., 2021; Sperling et al., 2014; Zait
336 et al., 2019) meaning that g_b was high. Because g_s is significantly smaller than g_b and since
337 resistances are summed ($\frac{1}{g_s} + \frac{1}{g_b}$), there is little impact of inaccuracy in g_b when resolving g_s
338 under high fan speed. For example, when measuring a leaf with a g_s of 0.2 mol m⁻² s⁻¹, changing
339 g_b from 2 mol m⁻² s⁻¹ to 3 mol m⁻² s⁻¹ would increase the overall conductance from 0.182 to 0.188
340 mol m⁻² s⁻¹. The estimation of g_b becomes far more important under low fan speed, when
341 inaccuracy in the g_b model could result in a significant impact on g_s estimation (see difference

342 between the blue and black lines in **Figs. 3 and 4**). It is thus critical to accurately estimate g_b
343 when measuring at low fan speeds.

344 *The effect of wind on stomatal mechanics and opening kinetics*

345 The effect of wind on stomatal conductance has important implications for determining stomatal
346 kinetics, understanding stomatal mechanics, and quantifying stomatal regulation in response to
347 environmental variables. It has long been known that the epidermal cells of angiosperms interact
348 with the guard cells to determine stomatal aperture (Darwin, 1898; Iwanoff, 1928) and several
349 studies demonstrated that equal loss of turgor in both guard and epidermal cells result in stomatal
350 opening (Glinka, 1971; Franks *et al.*, 1998; Franks & Farquhar, 2007). Our results suggest that
351 this guard cell and epidermal cell mechanical interaction influences the dynamics of stomatal
352 responses to both light and evaporative demand.

353 The most well-described manifestation of the epidermal interaction with the guard cells is the
354 wrong-way opening of stomata in response to leaf excision and rapid dehydration (Franks &
355 Farquhar, 2007; Zait *et al.*, 2017). This counter-intuitive response, wherein higher conductance
356 transiently occurs as leaf water status declines, can also occur at high VPD (Buckley *et al.*,
357 2011). The opening is thought to occur passively due to increase in transpiration, which leads to
358 lower turgor of both guard cells and epidermal cells and a corresponding increase in stomatal
359 aperture due to the mechanical advantage of epidermal cells (*ref.*). Our results, which showed a
360 similar effect of increased g_b to that of increased VPD_i , indicates that it is increased transpiration
361 that drives the rapid passive stomatal response to leaf water status via epidermal turgor, rather
362 than direct signaling induced by relative humidity or temperature (**Fig. 3**). This point is further
363 reinforced by the fact the VPD_i decrease with the increase in wind speed is reversible without
364 hysteresis (**Fig. 4, S2**). Our results align with those of Mott *et al.* (1990) showed that increased
365 transpiration due to exposing leaves to helox gas (2.3 times higher vapor diffusion relative to air)
366 also resulted in significant stomatal opening. This line of evidence suggests that the wrong-way
367 stomatal responses due to changes in transpiration are a mechanism by which angiosperms can
368 passively regulate stomata. However, the passive responses of angiosperm stomata are in the
369 opposite direction to the passive, “right-way” hydraulic regulation of stomatal responses to
370 changes in leaf water status observed in lycophytes and ferns (Brodribb and McAdam 2011).

371 From a quantitative perspective our data shows that relatively mild increases in transpiration
372 (from 2.2 to 3.2 $\text{mmol m}^{-2} \text{s}^{-1}$) results in a significant stomatal opening (from 0.3 to 0.5 mmol m^{-2}
373 s^{-1}). Since such transpiration increase can be driven by common environmental changes (e.g.
374 VPD increase from 1 to 2 kPa, a fairly common change for leaves that transition from shade to
375 sunlight, is expected to double transpiration) This highlights that many of the current stomatal
376 regulation models, which couples the extent and rate of stomatal movement only to ion transport,
377 are incomplete (Jezek *et al.*, 2019). Jezek *et al.* (2019) found that the stomatal opening kinetics
378 predicted by OnGuard models (focus on solute transport) were three-to-five times slower than in
379 vivo gas exchange observations. No parameter adjustments within physiological ranges brought
380 the model kinetics significantly closer to experimental data, indicating a missing component in
381 the model construction. The model prediction is in line with the stomatal opening that we have
382 documented in epidermal peels, highlighting that transpiration, and its passive effect on

383 epidermal turgor, could be the missing component. We suggest that integrating the transpiration
384 effect on stomatal regulation, as influenced by wind (or VPD) (**Fig. 7**) should improve the
385 model's ability to predict the actual kinetics of stomatal movement.

386 It should be noted that most past studies that exposed plants to higher wind speed found that they
387 exhibit lower g_s (e.g. Renard & Demessemaeker, 1983). This is probably the result of
388 unfavorable hydration conditions due to the higher transpiration, similar to the reduced g_s of
389 plants under high VPD (reference). This is not necessarily the case when a single leaf is placed
390 inside the gas exchange cuvette. The increased transpiration from a single leaf, has little impact
391 on whole plant water use and a negligible effect on xylem water potential. Accordingly, the
392 transpiration of a well hydrated leaf can be increased to some extent before it will lead to either
393 epidermal turgor loss, or loss of mesophyll cell turgor and the triggering of ABA biosynthesis
394 that might drive active stomatal closure (McAdam & Brodribb, 2016).

395 **Considerations for accurate g_s measurements**

396 The fact that wind speed has such a dramatic effect on g_s measurements, raises questions about
397 our ability to accurately estimate the native g_s . The effect is expected to be most pronounced
398 when leaves are taken from low-wind environments and placed in a gas exchange cuvette with
399 high fan speed that rapidly increase their transpiration and open their stomata, meaning that the
400 recorded value is higher than the native g_s . Most past studies have used high fan speed because
401 this is the official recommendation of gas exchange manufacturers, but it is a far more
402 complicated challenge to understand the wind speed that individual leaves experience in their
403 natural environment. Multiple studies report that the wind speed inside dense canopies of an
404 agricultural crop or forests are significantly lower than those measured by the meteorological
405 stations (typically located out of the field or forest; Shaw, 1977; Renaud et al., 2011). This
406 suggests that measuring leaves in conditions above their ambient wind, and consequently
407 inducing stomatal opening, is not rare. This notion is also supported by the fact that upscaling
408 leaf gas exchange measurements into canopy scale typically result in overestimation of the whole
409 plant transpiration (Flore, 2003; Hochberg et al., 2023).

410 Adjusting for potential artefacts requires careful consideration. Firstly, one should take into
411 account the ambient wind speed and direction and, in combination with the leaf dimensions,
412 determine the native g_b as suggested by Nobel (2020). Subsequently, adjusting the cuvette fan
413 speed helps in reproducing a similar boundary layer. However, it's noteworthy that in many
414 instances, users might be looking to assess gas exchange under standardized conditions rather
415 than the ambient (manifested in the common procedure to use a controlled temperature, CO_2
416 concentration, RH and fan speed).

417 To conclude, wind speed can have a large effect on stomatal conductance and stomatal kinetics.
418 Incorporating this effect into the current stomatal dogma and hydraulic models should improve
419 our ability to predict plant response to the environment. Accounting for the wind effect is critical
420 when measuring leaves using gas exchange system.

421 **Acknowledgment**

422 This study supported by the Israel Science Foundation (ISF) grant 2076/23 to Y.Z.

423

424 **References**

- 425 Aphalo, P. J., & Jarvis, P. G. (1993). The boundary layer and the apparent responses of stomatal
426 conductance to wind speed and to the mole fractions of CO₂ and water vapour in the air.
427 *Plant, Cell & Environment*, 16(7), 771–783. [https://doi.org/10.1111/j.1365-](https://doi.org/10.1111/j.1365-3040.1993.tb00499.x)
428 3040.1993.tb00499.x
- 429 Assmann, S. M., & Jegla, T. (2016). Guard cell sensory systems: recent insights on stomatal
430 responses to light, abscisic acid, and CO₂. *Current Opinion in Plant Biology*, 33, 157–167.
431 <https://doi.org/10.1016/j.pbi.2016.07.003>
- 432 Barzilai, O., Avraham, M., Sorek, Y., Zemach, H., Dag, A., & Hochberg, U. (2021). Productivity
433 versus drought adaptation in olive leaves: Comparison of water relations in a modern versus
434 a traditional cultivar. *Physiologia Plantarum*, 173(4), 2298–2306.
435 <https://doi.org/10.1111/ppl.13580>
- 436 Buckley, T. N. (2005). The control of stomata by water balance. *New Phytologist*, 168(2), 275–
437 292. <https://doi.org/10.1111/j.1469-8137.2005.01543.x>
- 438 Buckley, T. N., Sack, L., & Gilbert, M. E. (2011). The role of bundle sheath extensions and life
439 form in stomatal responses to leaf water status. *Plant Physiology*, 156(2), 962–973.
440 <https://doi.org/10.1104/pp.111.175638>
- 441 Cowan, I. R. (1978). Stomatal Behaviour and Environment. *Advances in Botanical Research*,
442 4(C), 117–228. [https://doi.org/10.1016/S0065-2296\(08\)60370-5](https://doi.org/10.1016/S0065-2296(08)60370-5)
- 443 Darwin, F. (1898). Observations on stomata. *Transactions of the Royal Society of London*,
444 58(1496), 212–213. <https://doi.org/10.1038/058212a0>
- 445 DeMichele, D. W., & Sharpe, P. J. H. (1973). An analysis of the mechanics of guard cell motion.
446 *Journal of Theoretical Biology*, 41(1), 77–96. [https://doi.org/10.1016/0022-5193\(73\)90190-](https://doi.org/10.1016/0022-5193(73)90190-2)
447 2
- 448 Flore, G. F. & J. A. (2003). Comparison Between Different Methods for Measuring
449 Transpiration in Potted Apple Trees. *Biologia Plantarum*, 46(1), 41–47.
- 450 Foster, J. R., & Smith, W. K. (1986). Influence of stomatal distribution on transpiration in
451 low-wind environments. *Plant, Cell & Environment*, 9(9), 751–759.
452 <https://doi.org/10.1111/j.1365-3040.1986.tb02108.x>
- 453 Franks, P. J. (2013). Passive and active stomatal control: Either or both? *New Phytologist*,
454 198(2), 325–327. <https://doi.org/10.1111/nph.12228>
- 455 Franks, P. J., Cowan, I. R., & Farquhar, G. D. (1998). A study of stomatal mechanics using the
456 cell pressure probe. *Plant, Cell and Environment*, 21(1), 94–100.
457 <https://doi.org/10.1046/j.1365-3040.1998.00248.x>
- 458 Franks, P. J., & Farquhar, G. D. (2007). The mechanical diversity of stomata and its significance
459 in gas-exchange control. *Plant Physiology*, 143(1), 78–87.
460 <https://doi.org/10.1104/pp.106.089367>

- 461 Frensch, J., & Schulze, E. D. (1988). The effect of humidity and light on cellular water relations
462 and diffusion conductance of leaves of *Tradescantia virginiana* L. *Planta*, *173*(4), 554–562.
463 <https://doi.org/10.1007/BF00958969>
- 464 Glinka, Z. (1971). The Effect of Epidermal Cell Water Potential on Stomatal Response to
465 Illumination of Leaf Discs of *Vicia faba*. *Physiologia Plantarum*, *24*(3), 476–479.
466 <https://doi.org/10.1111/j.1399-3054.1971.tb03521.x>
- 467 Hochberg, U., Perry, A., Rachmilevitch, S., Ben-Gal, A., & Sperling, O. (2023). Instantaneous
468 and lasting effects of drought on grapevine water use. *Agricultural and Forest Meteorology*,
469 *338*(May), 109521. <https://doi.org/10.1016/j.agrformet.2023.109521>
- 470 Iwanoff, L. (1928). Zur Methodik der Transpirationsbestimmung am Standort. *Ber Dtsch Bot*
471 *Ges*, *46*., 306–310. <https://doi.org/10.1007/BF00419279>
- 472 Jezek, M., Hills, A., Blatt, M. R., & Lew, V. L. (2019). A constraint–relaxation–recovery
473 mechanism for stomatal dynamics. *Plant Cell and Environment*, *42*(8), 2399–2410.
474 <https://doi.org/10.1111/pce.13568>
- 475 Kearns, E. V., & Assmann, S. M. (1993). The guard cell-environment connection. *Plant*
476 *Physiology*, *102*(3), 711–715. <https://doi.org/10.1104/pp.102.3.711>
- 477 Kim, T.-H., Böhmer, M., Hu, H., Nishimura, N., & Schroeder, J. I. (2010). Guard Cell Signal
478 Transduction Network: Advances in Understanding Abscisic Acid, CO₂, and Ca²⁺
479 Signaling. *Annual Review of Plant Biology*, *61*(1), 561–591.
480 <https://doi.org/10.1146/annurev-arplant-042809-112226>
- 481 Kollist, H., Nuhkat, M., & Roelfsema, M. R. G. (2014). Closing gaps: Linking elements that
482 control stomatal movement. *New Phytologist*. <https://doi.org/10.1111/nph.12832>
- 483 Mcadam, S. A. M., & Brodribb, T. J. (2016). *Linking Turgor with ABA Biosynthesis*:
484 *Implications for Stomatal Responses to Vapor Pressure Deficit across Land Plants 1* [
485 *OPEN*]. *171*(July), 2008–2016. <https://doi.org/10.1104/pp.16.00380>
- 486 McAdam, S. a M., & Brodribb, T. J. (2014). Separating active and passive influences on
487 stomatal control of transpiration. *Plant Physiology*, *164*(4), 1578–1586.
488 <https://doi.org/10.1104/pp.113.231944>
- 489 McNab, B. K. (2006). The relationship among flow rate, chamber volume and calculated rate of
490 metabolism in vertebrate respirometry. *Comparative Biochemistry and Physiology - A*
491 *Molecular and Integrative Physiology*, *145*(3), 287–294.
492 <https://doi.org/10.1016/j.cbpa.2006.02.024>
- 493 Meidner, H., & Heath, O. V. S. (1963). Rapid changes in transpiration in plants. In *Nature* (Vol.
494 200, Issue 4903, pp. 283–284). <https://doi.org/10.1038/200283a0>
- 495 Mott, K. a., & Franks, P. J. (2001). The role of epidermal turgor in stomatal interactions
496 following a local perturbation in humidity. *Plant, Cell and Environment*, *24*(6), 657–662.
497 <https://doi.org/10.1046/j.0016-8025.2001.00705.x>
- 498 Nobel, P. S. (2020). Physicochemical and environmental plant physiology. In *Physicochemical*
499 *and Environmental Plant Physiology* (5th ed.). Academic Press.

- 500 <https://doi.org/10.1016/C2018-0-04662-9>
- 501 Parkinson, K. J. (1985). A simple method for determining the boundary layer resistance in leaf
502 cuvettes. *Plant, Cell & Environment*, 8(3), 223–226. [https://doi.org/10.1111/1365-](https://doi.org/10.1111/1365-3040.ep11604618)
503 [3040.ep11604618](https://doi.org/10.1111/1365-3040.ep11604618)
- 504 Raschke, K. (1970). Leaf Hydraulic System: Rapid Epidermal and Stomatal Responses to
505 Changes in Water Supply. *Science*, 167, 189–191.
- 506 Renard, C., & Demessemacker, W. (1983). Effects of wind velocity on stomatal conductance and
507 consequences of leaf rolling on water uptake in tall fescue. *Biologia Plantarum*, 25(6), 408–
508 411. <https://doi.org/10.1007/BF02903136>
- 509 Renaud, V., Innes, J. L., Dobbertin, M., & Rebetez, M. (2011). Comparison between open-site
510 and below-canopy climatic conditions in Switzerland for different types of forests over 10
511 years (1998–2007). *Theoretical and Applied Climatology*, 105(1), 119–127.
512 <https://doi.org/10.1007/s00704-010-0361-0>
- 513 Shaw, R. H. (1977). Secondary Wind Speed Maxima Inside Plant Canopies. *Journal of Applied*
514 *Meteorology and Climatology*, 16(May), 514–521.
- 515 Shimazaki, K., Doi, M., Assmann, S. M., & Kinoshita, T. (2007). Light regulation of stomatal
516 movement. *Annual Review of Plant Biology*, 58, 219–247.
517 <https://doi.org/10.1146/annurev.arplant.57.032905.105434>
- 518 Sperling, O., Lazarovitch, N., Schwartz, A., & Shapira, O. (2014). Effects of high salinity
519 irrigation on growth, gas-exchange, and photoprotection in date palms (*Phoenix dactylifera*
520 L., cv. Medjool). *Environmental and Experimental Botany*, 99, 100–109.
521 <https://doi.org/10.1016/j.envexpbot.2013.10.014>
- 522 Zait, Y., Shapira, O., & Schwartz, A. (2017). The effect of blue light on stomatal oscillations and
523 leaf turgor pressure in banana leaves. *Plant, Cell & Environment*, 40(January), 1143–1152.
524 <https://doi.org/10.1111/pce.12907>
- 525 Zait, Y., Shtein, I., & Schwartz, A. (2019). Long-term acclimation to drought, salinity and
526 temperature in the thermophilic tree *Ziziphus spina-christi*: Revealing different tradeoffs
527 between mesophyll and stomatal conductance. *Tree Physiology*, 39(5), 701–716.
528 <https://doi.org/10.1093/treephys/tpy133>
- 529 Zhu, M., Jeon, B. W., Geng, S., Yu, Y., Balmant, K., & Chen, S. (2016). Preparation of
530 Epidermal Peels and Guard Cell Protoplasts for Cellular, Electrophysiological, and -Omics
531 Assays of Guard Cell Function. *Methods in Molecular Biology*, 1363(November), 89–121.
532 https://doi.org/10.1007/978-1-4939-3115-6_9

533

534 **Figure legends:**

535 **Figure 1:** Relationship between flow rate and CO₂ differential (respiration in the dark from a
536 mango leaf) inside the LI-6800 leaf chamber at four different fan speeds: 200 rpm (a), 800 rpm
537 (b), 2000 rpm (c), and 10000 rpm (d). The line represents the linear relationship between delta
538 CO₂ and flow rate where the chamber air mixing is above the critical flow rate point. The red

539 arrow represents the anticipated critical point below which air mixing is not sufficient. Data is
540 shown from a single flow rate curve for each fan speed (mean \pm SD from at least 20
541 measurements of ΔCO_2 , recorded at 10 s intervals after each flow rate stabilized.

542 **Figure 2:** Effect of fan speed on wind speed and boundary layer conductance inside the LI-
543 6800 chamber. Wind speed was measured using an omnidirectional hot wire sensor and
544 boundary layer conductance was estimated by the wet filter paper method. The measurements
545 were conducted under dark conditions, a filter paper temperature (T_{exchange}) of 22°C, and a leaf
546 vapor pressure deficit (VPD) ranging between 0.6-1 kPa. The black squares represent boundary
547 layer conductance calculated following the methodology outlined by Nobel at each wind speed
548 (2020). The purple triangles represent the boundary layer conductance calculated by the Licor
549 software at each fan speed. The red circles represent the boundary layer conductance of the filter
550 paper (mean \pm SD from four separate determinations), estimated as the total leaf conductance
551 calculated by the LI-6800 (gtw). The blue triangles represent the wind speed at the leaf plane
552 inside the chamber at each fan speed ((mean \pm SD from nine separate measurements).

553 **Figure 3:** The effect of a rapid increase from low (1000 rpm) to high (10000 rpm) fan speed on
554 *Arabidopsis*: (a) stomatal conductance (g_s) according to the boundary layer estimated by the LI-
555 6800 (black triangles) and after correcting the boundary layer conductance according to our
556 measurements (blue circles), and wind speed (red squares), and (b) transpiration (E, blue circles)
557 and leaf-to-air vapor pressure deficit (VPD_l , red circles). Measurements were carried out at a
558 CO_2 concentration of 100 ppm to minimize the effect of internal CO_2 concentration on stomatal
559 aperture.

560 **Figure 4:** The effect of gradual changes in wind speed on *Arabidopsis*: (a) stomatal conductance
561 (g_s) according to the boundary layer estimated by the LI-6800 (black triangles) and after
562 correcting the boundary layer values according to our measurements (blue circles), (b)
563 transpiration (E, blue circles) and leaf-to-air vapor pressure deficit (VPD_l , red squares), and (c)
564 photosynthesis (A, blue triangles) and transpiration efficiency (A/E, red circles) at ambient CO_2
565 (415 ppm). Wind speed was changed by adjusting the leaf fan speed from 200 rpm to 7000 rpm
566 over a period of five minutes. Data shown as mean \pm SE from four independent replications.

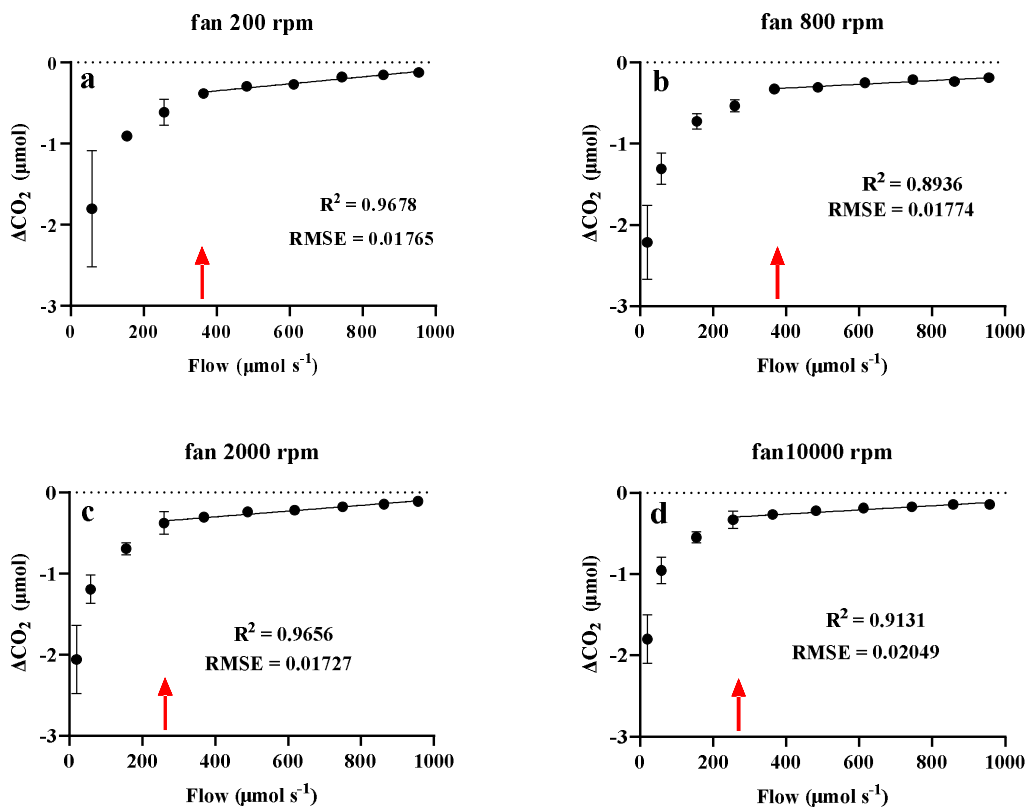
567 **Figure 5:** Changes in stomatal conductance throughout the transition from darkness to light (800
568 $\mu\text{mol m}^{-2} \text{s}^{-1}$) for leaves of *Vicia faba* subjected to fan speeds of 500, 1000, and 10000 rpm.
569 Additionally, the data illustrates variation in stomatal aperture observed in epidermal peels in a
570 buffer solution derived from leaves collected from the same plants. The data are expressed as a
571 percentage of stomatal opening $[(g_{s \text{ max}} - g_s) / g_{s \text{ max}}]$ to facilitate comparison between gas
572 exchange and epidermal peel measurements. Error bars represent the standard deviation from
573 three independent measurements (n=3).

574 **Figure 6:** The effect of wind speed within the LI-6800 chamber on stomatal conductance in
575 multiple plant species (corrected for boundary layer based on filter paper). Error bars represent
576 the standard deviation from three independent measurements (n=3). Inset shows the linear slopes
577 of the regression fit between g_s and wind speed \pm 95% CI.

578 **Figure 7: (a)** Illustration of low wind speed scenario. The boundary layer (BL) around the leaf is
579 relatively thick, impeding the diffusion of water vapor from the leaf surface to the external
580 environment, thereby slowing transpiration (represented by thinner blue arrows coming out of
581 the stomatal pores). **(b)** Condition of high wind speed. In this case, the increased air movement
582 disrupts and thus thins the boundary layer around the leaf. A thinner boundary layer facilitates
583 the diffusion of water vapor from the leaf surface to the external environment, accelerating
584 transpiration (indicated by thicker blue arrows). The increase in transpiration creates a greater
585 water deficit in the leaf tissues, leading to a decrease in turgor pressure within the epidermal
586 cells, especially those surrounding the stomata. This loss of turgor pressure passively causes the
587 stomata to open, facilitating further transpiration and allowing greater uptake of CO₂.

588

589

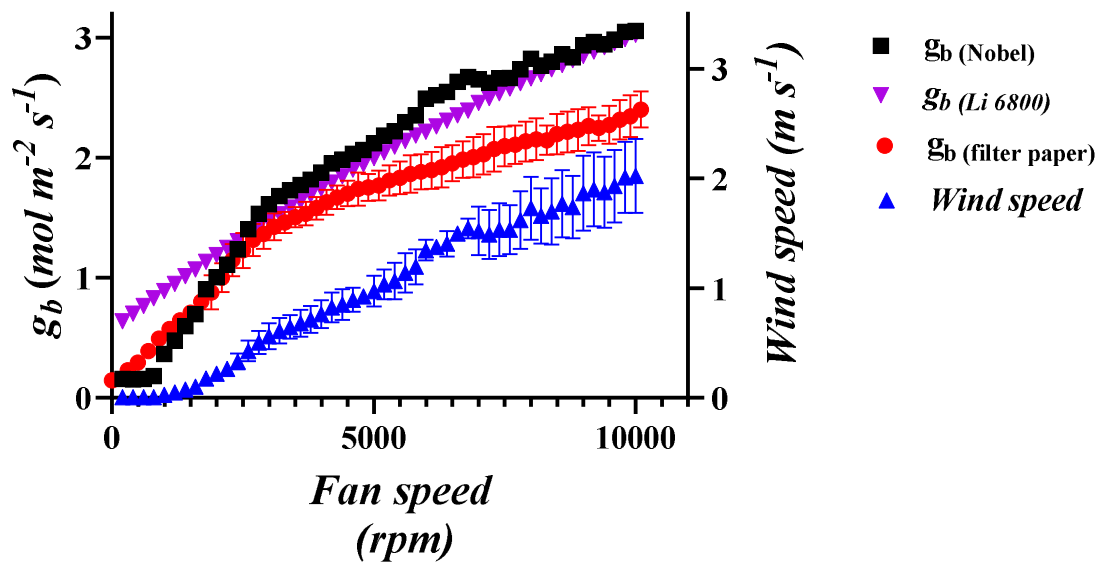


590

591 **Figure 1:** Relationship between flow rate and CO₂ differential (respiration in the dark from a
592 mango leaf) inside the LI-6800 leaf chamber at four different fan speeds: 200 rpm (a), 800 rpm
593 (b), 2000 rpm (c), and 10000 rpm (d). The line represents the linear relationship between delta
594 CO₂ and flow rate where the chamber air mixing is above the critical flow rate point. The red
595 arrow represents the anticipated critical point below which air mixing is not sufficient. Data is
596 shown from a single flow rate curve for each fan speed (mean ± SD from at least 20
597 measurements of ΔCO₂, recorded at 10 s intervals after each flow rate stabilized).

598

599



600

601 **Figure 2:** Effect of fan speed on wind speed and boundary layer conductance inside the LI-
602 6800 chamber. Wind speed was measured using an omnidirectional hot wire sensor and
603 boundary layer conductance was estimated by the wet filter paper method. The measurements
604 were conducted under dark conditions, a filter paper temperature (T_{exchange}) of 22°C, and a leaf
605 vapor pressure deficit (VPD) ranging between 0.6-1 kPa. The black squares represent boundary
606 layer conductance calculated following the methodology outlined by Nobel at each wind speed
607 (2020). The purple triangles represent the boundary layer conductance calculated by the Licor
608 software at each fan speed. The red circles represent the boundary layer conductance of the filter
609 paper (mean \pm SD from four separate determinations), estimated as the total leaf conductance
610 calculated by the LI-6800 (gtw). The blue triangles represent the wind speed at the leaf plane
611 inside the chamber at each fan speed ((mean \pm SD from nine separate measurements).

612

613

614

615

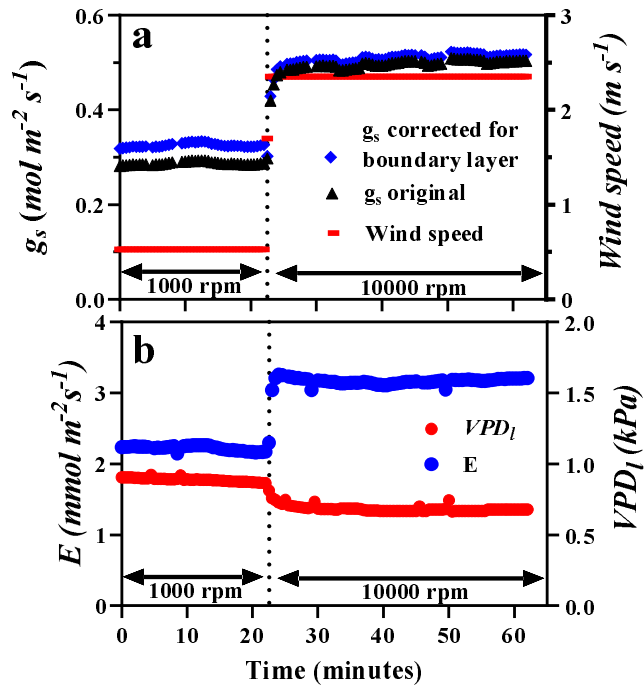
616

617

618

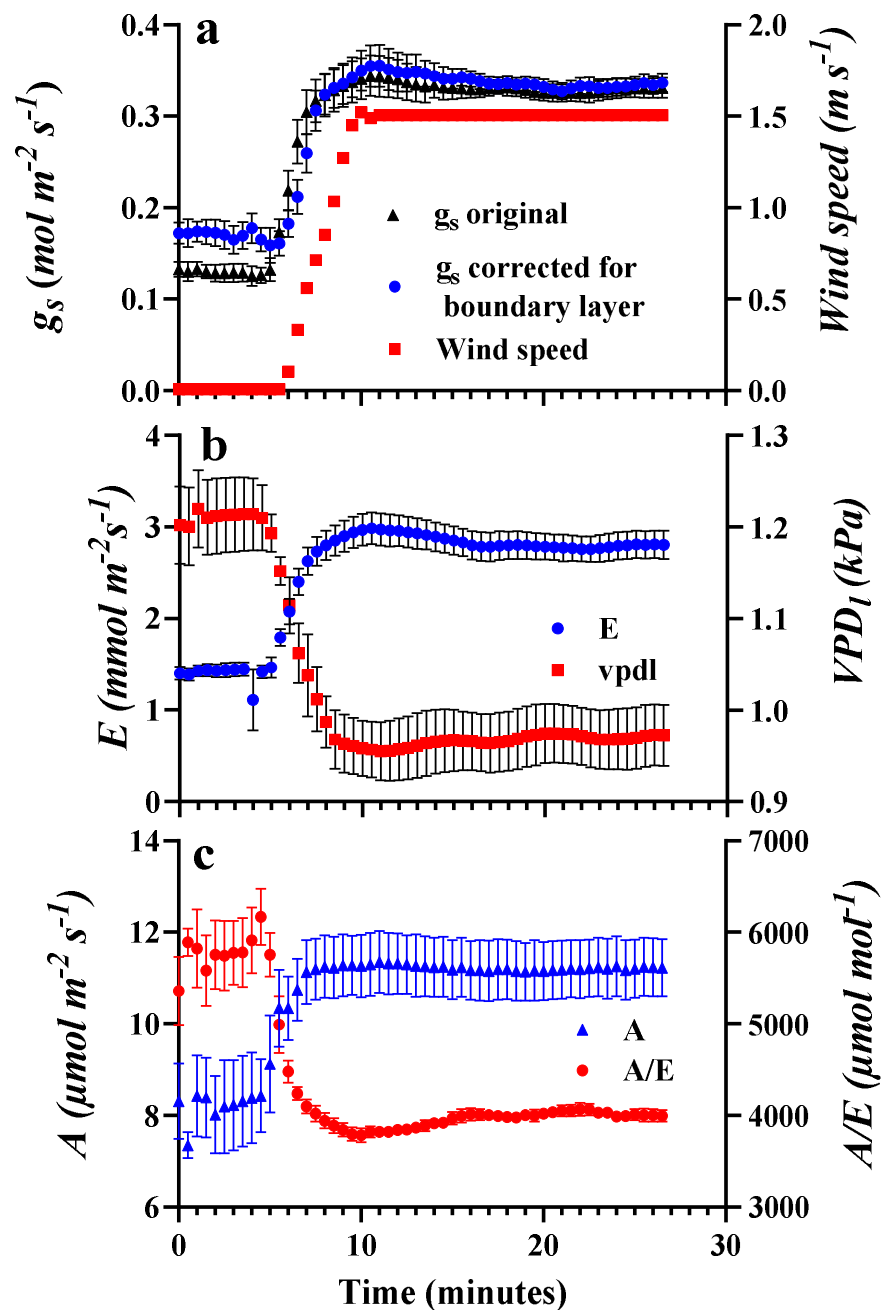
619

620
621
622
623
624



625
626
627
628
629
630
631
632
633

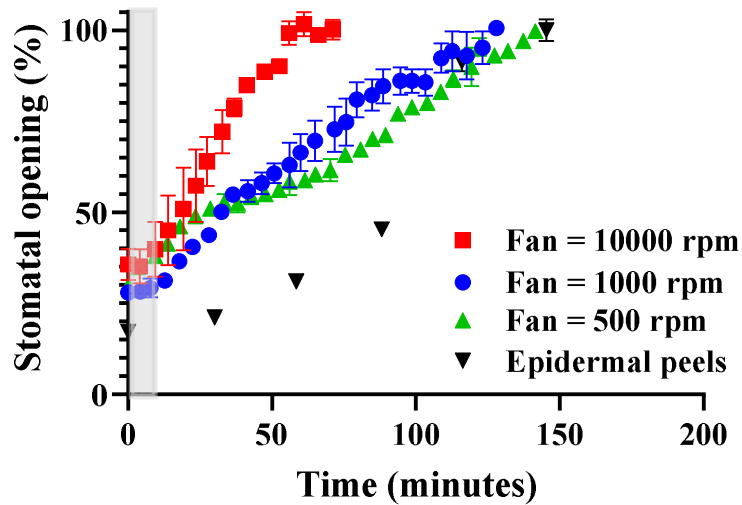
Figure 3: The effect of a rapid increase from low (1000 rpm) to high (10000 rpm) fan speed on Arabidopsis: (a) stomatal conductance (g_s) according to the boundary layer estimated by the LI-6800 (black triangles) and after correcting the boundary layer conductance according to our measurements (blue circles), and wind speed (red squares), and (b) transpiration (E , blue circles) and leaf-to-air vapor pressure deficit (VPD_l , red circles). Measurements were carried out at a CO_2 concentration of 100 ppm to minimize the effect of internal CO_2 concentration on stomatal aperture.



634

635 **Figure 4:** The effect of gradual changes in wind speed on Arabidopsis: (a) stomatal conductance
636 (g_s) according to the boundary layer estimated by the LI-6800 (black triangles) and after
637 correcting the boundary layer values according to our measurements (blue circles), (b)
638 transpiration (E , blue circles) and leaf-to-air vapor pressure deficit (VPD_l , red squares), and (c)
639 photosynthesis (A , blue triangles) and transpiration efficiency (A/E , red circles) at ambient CO_2
640 (415 ppm). Wind speed was changed by adjusting the leaf fan speed from 200 rpm to 7000 rpm
641 over a period of five minutes. Data shown as mean \pm SE from four independent replications.

642



643

644 **Figure 5:** Changes in stomatal conductance throughout the transition from darkness to light (800
645 $\mu\text{mol m}^{-2} \text{s}^{-1}$) for leaves of *Vicia faba* subjected to fan speeds of 500, 1000, and 10000 rpm.
646 Additionally, the data illustrates variation in stomatal aperture observed in epidermal peels in a
647 buffer solution derived from leaves collected from the same plants. The data are expressed as a
648 percentage of stomatal opening $[(g_{s \text{ max}} - g_s) / g_{s \text{ max}}]$ to facilitate comparison between gas
649 exchange and epidermal peel measurements. Error bars represent the standard deviation from
650 three independent measurements ($n=3$).

651

652

653

654

655

656

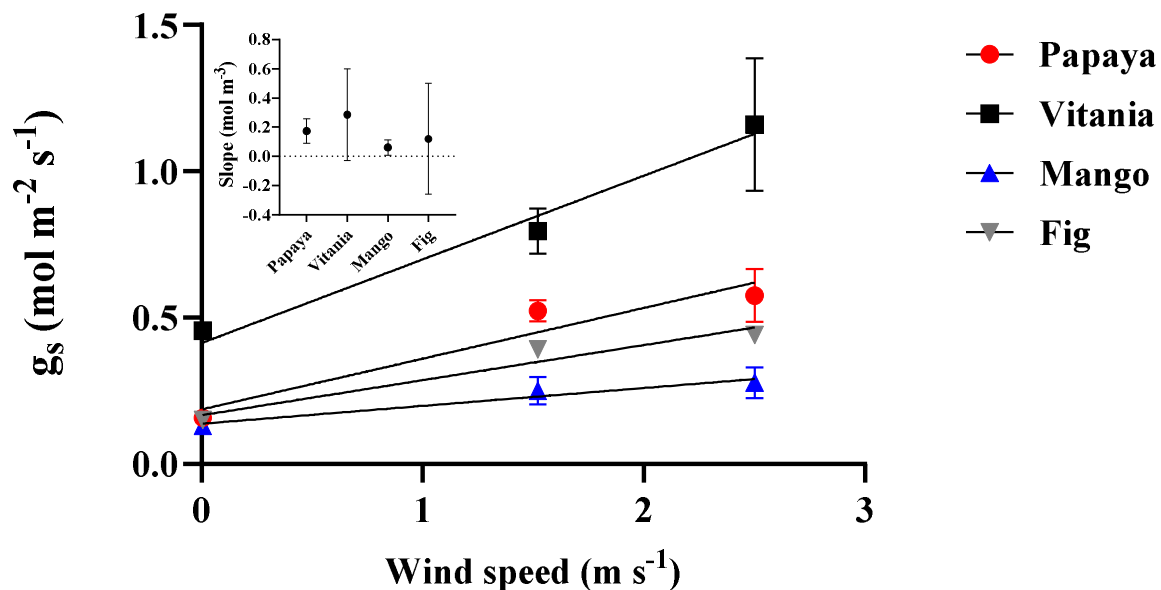
657

658

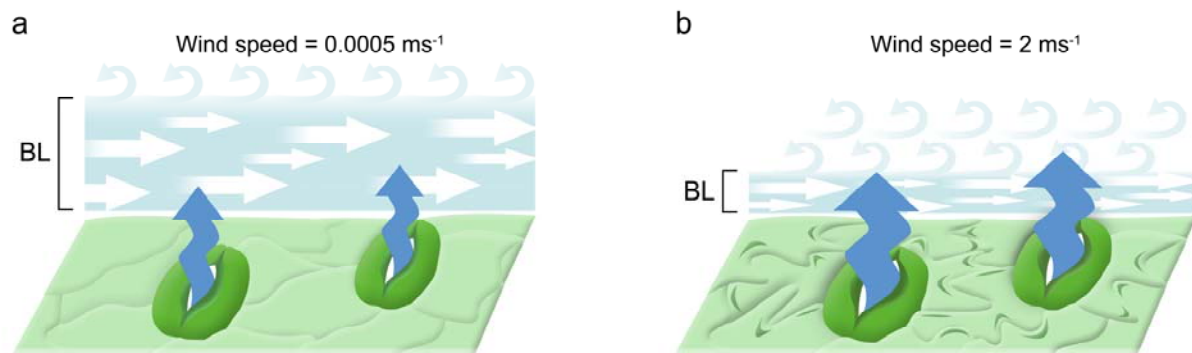
659

660

661



662
663 **Figure 6:** The effect of wind speed within the LI-6800 chamber on stomatal conductance in
664 multiple plant species (corrected for boundary layer based on filter paper). Error bars represent
665 the standard deviation from three independent measurements ($n=3$). Inset shows the linear slopes
666 of the regression fit between g_s and wind speed \pm 95% CI.



667
668 **Figure 7:** (a) Illustration of low wind speed scenario. The boundary layer (BL) around the leaf is
669 relatively thick, impeding the diffusion of water vapor from the leaf surface to the external
670 environment, thereby slowing transpiration (represented by thinner blue arrows coming out of
671 the stomatal pores). (b) Condition of high wind speed. In this case, the increased air movement
672 disrupts and thus thins the boundary layer around the leaf. A thinner boundary layer facilitates
673 the diffusion of water vapor from the leaf surface to the external environment, accelerating
674 transpiration (indicated by thicker blue arrows). The increase in transpiration creates a greater
675 water deficit in the leaf tissues, leading to a decrease in turgor pressure within the epidermal
676 cells, especially those surrounding the stomata. This loss of turgor pressure passively causes the
677 stomata to open, facilitating further transpiration and allowing greater uptake of CO_2 .

678

679

680

681

682

683

684

685

686

687

688

689

690

691

692

693